Optica Applicata, Vol. XLVIII, No. 2, 2018
DOI: 10.5277/oa180209

Demarcation energy properties of regenerated fiber Bragg grating sensors in few-mode fibers

NURUL ASHA MOHD NAZAL[1*], MAN-HONG LAI[1], KOK-SING LIM[1], DINUSHA SERANDI GUNAWARDENA[1], WU-YI CHONG[1], HANG-ZHOU YANG[2], HARITH AHMAD[1]

[1]Photonics Research Centre, University of Malaya, 50603 Kuala Lumpur, Malaysia

[2]School of Physics, Northwest University, Xi'an, Shaanxi 710069, China

[*]Corresponding author: n.asha2704@yahoo.com

In this work, thermal regeneration of fiber Bragg gratings inscribed in single-mode fibers, two-mode step index fibers and four-mode step index fibers is performed, where the single-mode fibers are used as the reference in the analysis. Specifically, we investigate the behavior of the thermal decay, recovery and eventually the permanent erasure of the gratings in the temperature range from 25 to 1300°C. In the domain of demarcation energy, the thermal responses of the gratings can be normalized and they share similar characteristic curves despite the different temperature ramping rates used in the annealing treatment. It is found that the demarcation energy at the regeneration point and the attempt-to-escape frequency for each grating can be associated with the confinement factors of the fibers. The finding in this work has provided a new insight in the manufacture of regenerated fiber Bragg grating sensors by using few-mode fibers for multiparameter sensing in high temperature environments.

Keywords: regenerated fiber Bragg grating, thermal regeneration, thermal decay, few-mode fibers.

1. Introduction

Fiber Bragg gratings (FBGs) have been widely employed in many applications particularly in communication, laser generation and industrial sensing. Taking advantage of its sensitivity to strain and temperature, FBGs are one of the most commonly used and deployed optical sensors. In recent years, FBG-based temperature sensors have been developed and different approaches for their enhancement have been reported, for example regenerated fiber Bragg grating (RFBG) [1]. RFBGs provide stable gratings at extreme temperature conditions up to 1400°C. RFBGs have been found promising in terms of robustness and stability in the reflectivity and Bragg wavelength in ultra-high temperature environment. Nevertheless, there is a continuous effort in improving the durability and high reflectivity of the RFBGs in various approaches; for example, in the investigation of fibers with different dopants [2], fabrication and characterization

techniques [3], fiber photosensitization method [4] and irradiation laser wavelengths for grating inscription [5].

The properties of RFBGs in dynamic environments still require more exploration because it is believed that the operation of an RFBG beyond glass transition temperature T_g may result in hysteresis of the temperature response [6]. Besides, the mechanical strength of FBG will be weakened and result in brittleness after undergoing annealing at extreme temperatures [7], which leads to short lifespan and low reflectivity. It is believed that crystallization occurs in the grating during the thermal regeneration process [8]. The crystallization is responsible for brittleness [9] and increased attenuation [10] in the regenerated grating. Consequently, the increased attenuation in the grating leads to a decrease in the reflectivity [11]. These problems can be resolved by performing annealing at considerably lower temperatures or with reduced annealing time. In addition, it is important to understand the impact of cooling rate on the sensitivity and hysteresis of the RFBG behavior. The regeneration temperature can be associated with the glass transition temperature T_g which is different for fibers with different doping materials [3].

Much effort in research has been directed towards improving the performance of RFBGs in terms of reflectivity, manufacturing time, maximum temperature sustainability and wavelength stability. Bandyopadhyay *et al*. [12] have presented ultra-high temperature regenerated gratings over 1000°C in boron-codoped germanosilicate optical fiber using 193 nm ArF excimer laser. Canning *et al*. have explained the mechanism of regenerated gratings by proposing an alternative model involving crystallization of the vitreous state [7]. Yang *et al*. have demonstrated thermal regeneration on new glass composition-based photosensitive fiber temperature up to 1400°C [2]. In line with the development in exploring and studying the RFBGs, a new fabrication technique using direct CO_2 laser annealing has been demonstrated [3]. Unlike the conventional annealing procedure that is based on a hot oven, CO_2 laser annealing has overcome the problems of degradation in the mechanical strength of the fiber due to a rigid/slow ramp rate of annealing temperature in the conventional method. Besides single mode fibers (SMF), the thermal regeneration of the gratings in few mode fibers (FMFs) has been reported [1]. High temperature annealing has been performed on two and four modes graded index FBG using a programmable high temperature tube furnace. Generally, there are large numbers of paths available for light propagation in multimode fibers (MMF). The core diameter and the difference between the refractive indices of the core and cladding of MMF are large compared to SMF [13]. In comparison with the standard MMFs, FMFs have higher resistance to cross-talk due to mode coupling while still possessing larger mode capacity than SMFs [14]. Thus, these fibers have less nonlinearity but give similar potential in terms of dispersion and attenuation as SMF. Apart from their unique advantages such as cost effectiveness, high sensitivity and discrimination capability [15], FMF based sensors can provide more capacity and flexibility than the SMF counterpart [16]. Since the fabrication process of FMF is compatible with standard SMF, this makes FMF an ideal candidate for long range sensing.

In the analysis of the RFBG, the thermal decay properties of the gratings can be characterized and well-predicted in the demarcation energy domain [17]. This technique has been proposed by ERDOGAN *et al*. to study the decay mechanisms by using accelerated aging data (the aging curve and the power law approach) [18]. RATHJE *et al*. have presented a novel continuous isochronal annealing method to obtain the aging curve for investigating the long term stability of the UV Bragg gratings that has been written in D_2 loaded and nonloaded fibers. The report shows that decays with various energy distributions can be analyzed with this isochronal annealing method [19]. In addition to the decay in grating strength, a shift in Bragg wavelength of boron-germanium codoped silica fiber has also been modeled according to an accelerated aging approach by PAL *et al*. It is shown that the temperature-induced irreversible shift in the Bragg wavelengths could not be predicted by use of an isothermal decay method [20].

In this work, the continuous isochronal annealing experiment has been performed on gratings inscribed in four mode step-index (4S) and two mode step-index (2S) fibers and SMFs by using a high temperature tube furnace and demarcation energy E_d is applied as characterization technique. Comparison of regeneration characteristics between three different types of fibers are observed at three different temperature ramping rates. The thermal responses of these gratings are presented in the domain of demarcation energy E_d. The extracted parameters are compared and discussed.

2. Methods

Two mode step-index (2S) (core diameter 19 μm) and four mode step-index (4S) (core diameter 25 μm) fibers supplied by OFS, Denmark, and single mode fibers (OFS ZWP -SMFs) (core diameter 8 μm) were soaked in a highly pressurized hydrogen gas chamber (13.8 MPa) for 2 weeks. Afterwards, 2 cm long grating structures were inscribed in the fibers by exposing them to 193 nm ArF excimer laser with the aid of a phase mask. The FBGs were then left at room temperature for more than 7 days to remove the residue hydrogen. The FMFs were spliced with SMF before the thermal annealing process. Subsequently, the gratings were inserted into a tube furnace (LT Furnace STF25/150-1600) and continuous isochronal thermal annealing procedure was carried out which was initiated from room temperature, 25°C, up to 1300°C. A linear temperature ramping procedure was carried out at a rate of 3°C/min. During the process, the grating reflectivity rapidly decays until it is erased followed by a progressive regeneration. As the annealing temperature continues to increase, the reflectivity of the produced RFBG begins to decay again until it is permanently erased at a temperature of about 1100°C. The thermal decay and thermal regeneration of the peak reflectivity are determined from the Bragg transmission loss (BTL) of the gratings. Throughout the whole annealing process, the transmission spectrum was monitored by an optical spectrum analyzer (OSA) and recorded continuously using LabVIEW software via a GPIB interface card. The experimental setup is illustrated in Fig. 1. The thermal decay of the grating reflectivity at each minute was represented in terms of the normalized integrat-

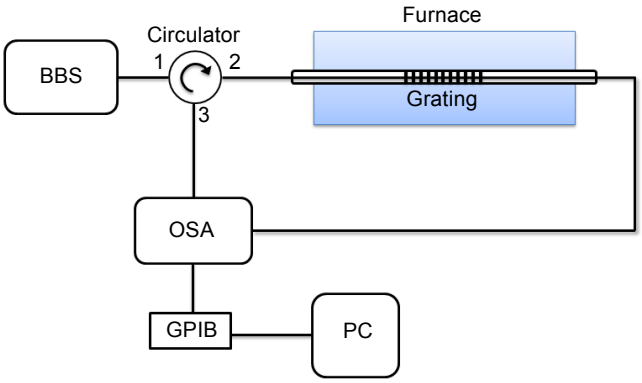

Fig. 1. The experimental setup of the annealing process using a high temperature tube furnace. BBS – broadband source, OSA – optical spectrum analyzer, GPIB – general purpose interface bus, PC – personal computer.

ed coupling coefficient (NICC) η as it is directly related to the refractive index modulation Δn_{mod} whereas the effective refractive index Δn_{eff} of the fiber is responsible for the Bragg wavelength shift [20].

The NICC was obtained by normalizing the integrated coupling coefficient (ICC) to its initial value,

$$\text{ICC} = \tanh^{-1}\sqrt{R} \tag{1}$$

where R is the grating reflectivity.

With reference to Eq. (1), the ICC is directly proportional to the peak reflectivity. Therefore, NICC can be expressed as follows:

$$\text{NICC} = \frac{\tanh^{-1}\sqrt{R_{t,\,T}}}{\tanh^{-1}\sqrt{R_{0,\,T_0}}} \tag{2}$$

where $R_{t,\,T}$ is the peak reflectivity after an annealing time t at annealing temperature T and $R_{0,\,T_0}$ is the reflectivity before annealing at room temperature [21].

The procedure was repeated at different ramping rates of 6 and 9°C/min as well.

3. Results and discussion

The results of the isochronal annealing process are presented in Fig. 2 for SMF, 2S and 4S fibers at three different ramping rates. The figure represents the evolution of the grating strength of the fibers at ramping rates of 9, 6 and 3°C/min. Generally, the grating strength (NICC) rapidly decays until it is diminished at the regeneration point followed by a continuous recovery. As the annealing temperature continues to rise, the grating reflectivity begins to decay again and eventually it is completely erased within the temperature ranges of about 1100°C to 1200°C for SMF (Fig. 2**a**), about 1100°C

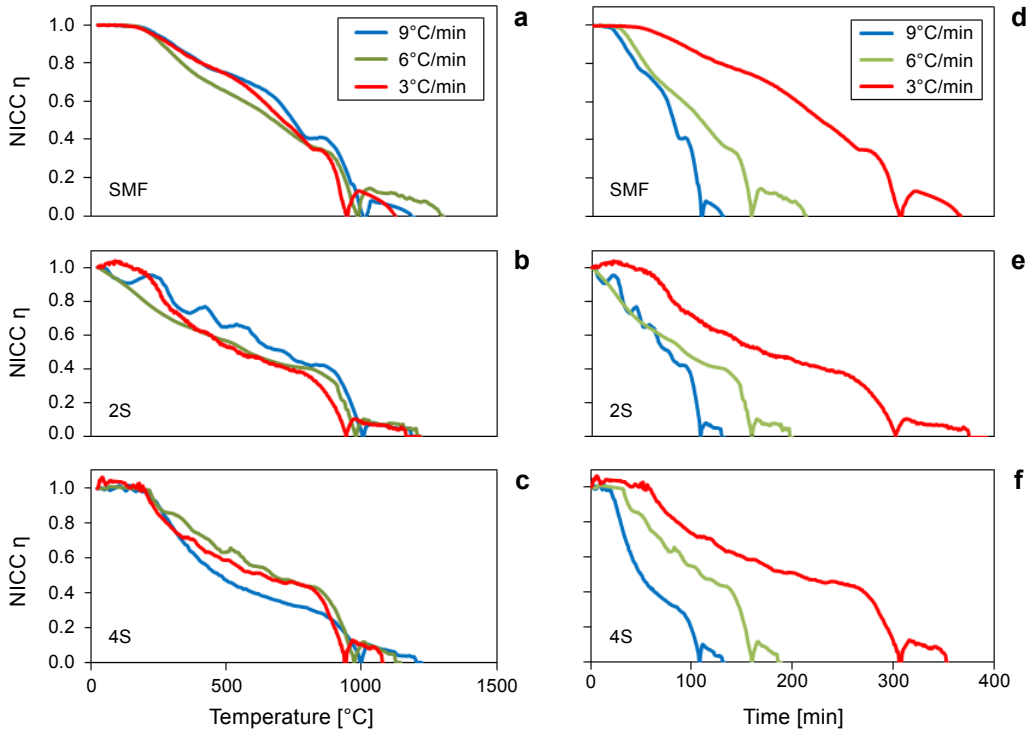

Fig. 2. Thermal decay characteristics of SMF (**a**, **d**), 2S (**b**, **e**) and 4S (**c**, **f**) at different ramping rates.

to 1200°C for 2S (Fig. 2**b**) and about 1070°C to 1200°C for 4S (Fig. 2**c**). The regeneration temperature is associated with the glass transition temperature T_g. Fibers with lower T_g have lower thermal regeneration temperature [3]. The experimental results indicate that the regeneration temperatures for these fibers are in a similar range of values as tabulated in the Table. It is worth noting that all three fibers used in the current study have the same numerical aperture N (see the Table), which indicates that their

T a b l e. Summarized comparison between SMF, 2S and 4S; RR denotes the ramping rate.

		SMF	2S	4S
Numerical aperture N		0.12	0.12	0.12
Core radius d [μm]		4	9.5	12.5
V number		1.95	4.63	6.09
Confinement factor Γ		0.488	0.843	0.903
Attempt-to-escape frequency ν [Hz]		3.2×10^5	8.0×10^5	1.0×10^6
Demarcation energy at regeneration temperature E_d [eV]		2.4	2.45	2.48
Regeneration temperature [°C]	RR = 3°C/min	941	943	946
	RR = 6°C/min	973	979	985
	RR = 9°C/min	997	997	997

cores share similar doping concentrations. Note that the regeneration temperature differs for different ramping rates. Fibers with lower ramping rates give lower value of regeneration temperature and *vice versa*. On the other hand, shorter regeneration time could be achieved by using a higher temperature increment rate [3]. From the experiment, a temperature ramping rate of 9°C/min requires over an hour to achieve the highest regeneration reflectivity, while both 6 and 3°C/min consume longer time which are more than 2 and 5 hours, respectively, for each type of fiber (refer Figs. 2**d**–2**f**).

The confinement factor Γ of the fiber can be expressed in a function of fiber core diameter d, numerical aperture N, and wavelength λ

$$\Gamma = \frac{\pi^2 d^2 N^2}{\lambda^2 + \pi^2 d^2 N^2} \tag{3}$$

The confinement factors of the SMF, 2S and 4S fiber used are 0.488, 0.843 and 0.903, respectively. The 4S fiber has the highest confinement factor, which means that the fraction of power flowing in the core is also the highest compared to the other two fibers. This finding is useful for understanding the properties that are related to the core diameter of RFBG sensors, particularly in FMFs.

The decay of the grating at any time t and temperature T is presented as a function of an aging parameter, and the demarcation energy E_d [18]

$$E_d = k_B T \ln(vt) \tag{4}$$

where k_B is the Boltzmann's constant and v is the attempt-to-escape frequency which can be obtained by overlapping the data sets of different ramping rates to best fit as a single curve through an iterative process. Figure 3 depicts the aging curves of three different types of fiber (SMF, 2S and 4S). In order to obtain the best-fit attempt-to-escape frequency v and demarcation energy E_d, three grating decays with different heating rates were fitted until the point at minimum NICC η coincide with each other in the same graph. In this study the thermal decay and recovery characteristics of SMFs and FMFs are analyzed in the demarcation energy domain which can be adhered as a useful characterization technique to predict the grating decay and recovery behavior with minimum dependence on the minimum temperature ramping rate. From the fitted curve (Fig. 3), the demarcation energies E_d at regeneration point (where the decay rate is maximum) for 4S, 2S and SMF are 2.48, 2.45 and 2.4 eV, respectively. The values for v were acquired as 1.0×10^6, 8.0×10^5 and 3.2×10^5 Hz for 4S, 2S and SMF, respectively [18]. The results show that FMFs have higher E_d and this means FMFs require higher energy to erase out the gratings to reach a complete decay before it starts to recover back compared to SMF. Therefore, FMFs need higher release rates for thermal depopulation of the traps at a given temperature T for a certain time t than SMF. During the annealing process, defects in lower demarcation energy transform to a higher demarcation energy state when the demarcation energy at the regeneration point is exceeded. This behavior results in the typical grating degradation and progressive recovery observed in Figs. 2 and 3 during thermal regeneration process. After a while,

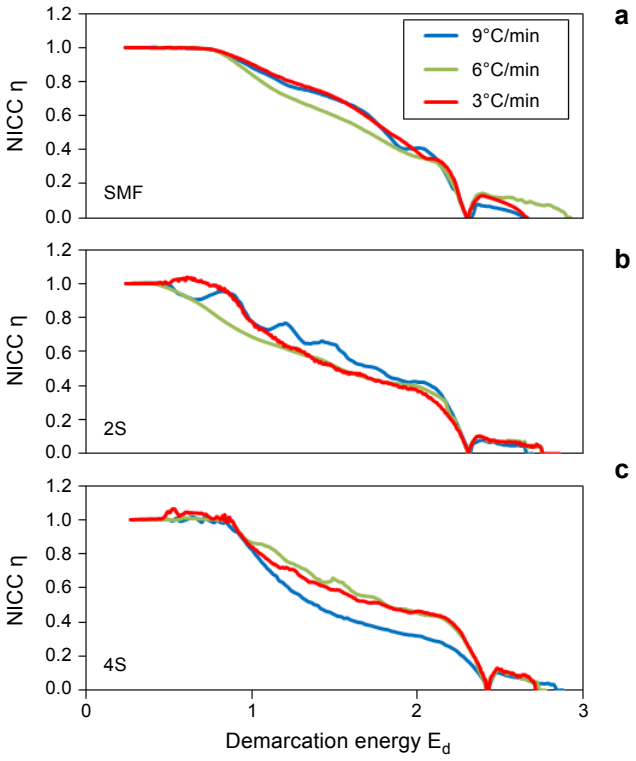

Fig. 3. NICC η *versus* demarcation energy E_d of SMF (**a**), 2S (**b**) and 4S (**c**) at different ramping rates.

the grating reaches its maximum reflectivity and starts to decay back leading to permanent erasure. At this time, the deformation of the grating occurs. The results show that the fiber with a larger confinement factor has higher demarcation energy at regeneration temperature and attempt-to-escape frequency. This can be attributed to the fact that the thermal regeneration mainly takes place in the fiber core where the grating structure is present.

4. Conclusion

The thermal regeneration of two mode step-index (2S) and four mode step-index (4S) fiber using a high temperature tube furnace has been demonstrated and demarcation energy is proposed as a characterization technique. The acquired characteristic curves of the thermal decay, recovery and permanent erasure of the gratings were presented in the temperature and time domains (see Fig. 2) and demarcation energy domain (see Fig. 3). The data presented in Fig. 3 represent the standardized form of the aging curves in the temperature and time domains. Regardless of the ramp rates used in the annealing process, the curves share similar decay characteristics in the demarcation energy domain. This technique can serve as a normalization process to ease the analysis and prediction of the thermal decay and regeneration of the grating during the annealing treatment.

The characteristic parameters of the RFBGs in SMF, 2S and 4S were obtained and compared. In this paper, the demarcation energy E_d and v have been associated with the confinement factor Γ of the fibers. The results show that 4S (highest Γ) yields the highest v and demarcation energy E_d. These findings are very important to study the complete system and to determine the optimum annealing condition for producing RFBG in the efficient manner in terms of manufacturing time, grating reflectivity and mechanical strength [22]. Furthermore, each ramping rate shows different regenerated temperature. Fibers with lower ramping rates give a lower regeneration temperature and *vice versa*. However, lower ramping rate required longer time for the regeneration process. By using a higher ramping rate, the fabrication of RFBG sensors can be achieved in a shorter period of time. The results from this work have provided a new insight in the manufacture of RFBG sensors by using FMF for sensing in extreme temperature environment.

Acknowledgements – We would like to thank UMRG (RG326-15AFR) and PRGS (PR001-2015A) for funding this project.

References

[1] Man-Hong Lai, Gunawardena D.S., Kok-Sing Lim, Machavaram V.R., Say-Hoe Lee, Wu-Yi Chong, Yen-Sian Lee, Ahmad H., *Thermal activation of regenerated fiber Bragg grating in few mode fibers*, Optical Fiber Technology 28, 2016, pp. 7–10.

[2] Hang Zhou Yang, Xue Guang Qiao, Das S., Paul M.C., *Thermal regenerated grating operation at temperatures up to 1400°C using new class of multimaterial glass-based photosensitive fiber*, Optics Letters 39(22), 2014, pp. 6438–6441.

[3] Man-Hong Lai, Gunawardena D.S., Kok-Sing Lim, Hang-Zhou Yang, Ahmad H., *Observation of grating regeneration by direct CO_2 laser annealing*, Optics Express 23(1), 2015, pp. 452–463.

[4] Cook K., Li-Yang Shao, Canning J., *Regeneration and helium: regenerating Bragg gratings in helium-loaded germanosilicate optical fibre*, Optical Materials Express 2(12), 2012, pp. 1733–1742.

[5] Barrera D., Sales S., *High-temperature optical sensor based in high birefringence regenerated FBGs and a simple interrogation scheme*, Proceedings of SPIE 8794, 2013, article ID 87941K.

[6] Man-Hong Lai, Kok-Sing Lim, Gunawardena D.S., Hang-Zhou Yang, Wu-Yi Chong, Ahmad H., *Thermal stress modification in regenerated fiber Bragg grating via manipulation of glass transition temperature based on CO_2-laser annealing*, Optics Letters 40(5), 2015, pp. 748–751.

[7] Canning J., Stevenson M., Bandyopadhyay S., Cook K., *Extreme silica optical fibre gratings*, Sensors 8(10), 2008, pp. 6448–6452.

[8] Lindner E., Chojetztki C., Brueckner S., Becker M., Rothhardt M., Vlekken J., Bartelt H., *Arrays of regenerated fiber Bragg gratings in non-hydrogen-loaded photosensitive fibers for high -temperature sensor networks*, Sensors 9(10), 2009, pp. 8377–8381.

[9] Nagendra N., Ramamurty U., Goh T.T., Li Y., *Effect of crystallinity on the impact toughness of a La-based bulk metallic glass*, Acta Materialia 48(10), 2000, pp. 2603–2615.

[10] Jiafang Bei, Monro T.M., Hemming A., Ebendorff-Heidepriem H., *Reduction of scattering loss in fluoroindate glass fibers*, Optical Materials Express 3(9), 2013, pp. 1285–1301.

[11] Gunawardena D.S., Man-Hong Lai, Kok-Sing Lim, Ali M.M., Ahmad H., *Measurement of grating visibility of a fiber Bragg grating based on bent-spectral analysis*, Applied Optics 54(5), 2015, pp. 1146–1151.

[12] BANDYOPADHYAY S., CANNING J., STEVENSON M., COOK K., *Ultrahigh-temperature regenerated gratings in boron-codoped germanosilicate optical fiber using 193 nm*, Optics Letters 33(16), 2008, pp. 1917–1919.
[13] NAIDU M., *Engineering Physics*, Pearson Education India, 2013.
[14] FATIH YAMAN, NENG BAI, BENYUAN ZHU, TING WANG, GUIFANG LI, *Long distance transmission in few-mode fibers*, Optics Express 18(12), 2010, pp. 13250–13257.
[15] VENGSARKAR A.M., MICHIE W.C., JANKOVIC L., CULSHAW B., CLAUS R.O., *Fiber-optic dual-technique sensor for simultaneous measurement of strain and temperature*, Journal of Lightwave Technology 12(1), 1994, pp. 170–177.
[16] AN LI, YIFEI WANG, QIAN HU, SHIEH W., *Few-mode fiber based optical sensors*, Optics Express 23(2), 2015, pp. 1139–1150.
[17] GUNAWARDENA D.S., MAN-HONG LAI, KOK-SING LIM, AHMAD H., *Thermal decay analysis of fiber Bragg gratings at different temperature annealing rates using demarcation energy approximation*, Optical Fiber Technology 34, 2017, pp. 16–19.
[18] ERDOGAN T., MIZRAHI V., LEMAIRE P.J., MONROE D., *Decay of ultraviolet-induced fiber Bragg gratings*, Journal of Applied Physics 76(1), 1994, pp. 73–80.
[19] RATHJE J., KRISTENSEN M., PEDERSEN J.E., *Continuous anneal method for characterizing the thermal stability of ultraviolet Bragg gratings*, Journal of Applied Physics 88(2), 2000, pp. 1050–1055.
[20] PAL S., MANDAL J., TONG SUN, GRATTAN K.T.V., *Analysis of thermal decay and prediction of operational lifetime for a type I boron-germanium codoped fiber Bragg grating*, Applied Optics 42(12), 2003, pp. 2188–2197.
[21] GUNAWARDENA D.S., MAN-HONG LAI, KOK-SING LIM, MALEKMOHAMMADI A., AHMAD H., *Fabrication of thermal enduring FBG sensor based on thermal induced reversible effect*, Sensors and Actuators A: Physical 242, 2016, pp. 111–115.
[22] TAO WANG, LI-YANG SHAO, CANNING J., COOK K., *Temperature and strain characterization of regenerated gratings*, Optics Letters 38(3), 2013, pp. 247–249.

Received June 3, 2017
in revised form August 23, 2017